Modeling of indoor air treatment using an innovative photocatalytic luminous textile: Reactor compactness and mass transfer enhancement

M. Abidi, A. Hajjaji, A. Bouzaza, L. Lamaa, L. Peruchon, C. Brochier, S. Rtimi, D. Wolbert, B. Bessais, Aymen Amin Assadi

Modeling of indoor air treatment using an innovative photocatalytic luminous textile: reactor compactness and mass transfer enhancement

Mabrouk Abidi[1,2,3], Anouar Hajjaji[1], Abdelkrim Bouzaza[2], Lina Lamaa[5], Laure Peruchon[5], Cédric Brochier[5], Sami Rtimi[4], Dominique Wolbert[2], Brahim Bessais[1], Aymen Amin Assadi[2]*

[1]Laboratoire de Photovoltaïque, Centre de Recherches et des Technologies de l'Energie, Technopole de Borj-Cédria, BP 95, 2050 Hammam-Lif, Tunisia

[2]Univ Rennes, Ecole Nationale Supérieure de Chimie de Rennes, CNRS, ISCR (Institut des Sciences Chimiques de Rennes), UMR 6226, F-35000 Rennes, France

[3] Faculté des sciences de Tunis, Université de Tunis El Manar, BP 94, Rommana, 1068 Tunis, Tunisia

[4]Ecole Polytechnique Fédérale de Lausanne (EPFL), EPFL-STI-IMX-LTP, Station 12, CH-1015, Lausanne, Switzerland

[5]Brochier Technologies, 90 Rue Frédéric Fays, 69100 Villeurbanne Lyon, France.

*Corresponding author: E-mail addresses: aymen.assadi@ensc-rennes.fr (A.A. Assadi)

Abstract

Indoor air pollution is a complex problem that involves a wide range and diversity of pollutants that threaten human health. In this context, significant efforts must be made to improve the quality of indoor air. It is therefore important to start controlling the sources of indoor pollution. However, where eliminating or minimizing sources of emissions is not technically feasible, technologies to reduce them should be used. The present work deals with the photocatalytic depollution of hospitals indoor air, using a continuous photocatalytic process. In order to get closer to real conditions, two model pollutants representing the indoor air of hospitals were chosen as targets; chloroform ($CHCl_3$) and glutaraldehyde ($C_5H_8O_2$). The photocatalytic oxidation of VOCs alone and their mixture (binary mixing

system) has been studied on a pilot scale. Indeed, the experiments were carried out in a continuous planar reactor using a new technology based on the TiO_2 / optical fiber photocatalyst.

The effects of experimental conditions such as air flow rate (4 - 12 $m^3.h^{-1}$), VOCs inlet concentration (4 - 40 $mg.m^{-3}$) and humidity levels (5 - 90%) were pointed out. The photocatalytic effect of the OF-TiO_2 composite was found to be improved under UV irradiation as compared to TiO_2. The presence of water molecules in small amounts (less than RH =30 %) can promote the degradation process due to the formation of $^{\bullet}OH$ radicals. Biomolecular Langmuir-Hinshelwood model including mass transfer step has been developed to represent the process behavior. Reusability test show that the optical fiber - based photocatalysts presented good photocatalytic activities towards $CHCl_3$/$C_5H_8O_2$ removal.

Keywords:

Indoor air treatment, luminous textiles, photocatalytic reactor, kinetic modelling, Mass transfer

Introduction

It is well known that we spend more than 80% of our time in closed spaces such as housing, workplace, school ..., and the air we breathe is not always of good quality [1, 2]. In addition to the supply of outside air, there are many potential sources of pollution in buildings: combustion devices, building materials, decorative products (paint, glues, varnishes, etc.), furniture, and human activity (smoking, maintenance of products, cooking, etc.). Inside, the air is really polluted in a specific way compared to the outside air. As a result, in recent decades, the prevalence of Sick Building Syndrome (SBS), Building Related Illness (BRI) and Multiple Chemical Sensitivity (MCS) have been reported, making Indoor Air Quality (IAQ) a major concern [3-7]. Indoor air pollutants (IAPs) mainly include carbon monoxide (CO), microorganisms (fungi, bacteria and viruses), nitrogen oxides (NOx) and a large variety of volatile organic compounds (VOCs). Photocatalytic oxidation is a promising technology for removing volatile organic compounds (VOCs) during indoor air treatment [5, 6]. The photocatalytic process has been of great interest in removing VOCs from indoor air as it has proven its effectiveness at room temperature, also for its low cost and its harmlessness [8]. Photocatalytic oxidation involves an interaction between the photocatalyst, light and the pollutant. Indeed, the photocatalyst must be excited by light irradiation and the pollutant must be adsorbed on the photocatalyst surface to be removed [8-12]. The practical application of metal oxide semiconductors as photocatalysts generally requires placing the photocatalyst in a configuration which allows it to be used continuously for the treatment of air. In conventional reactors, the photocatalyst is attached to the walls of the reactor by a support or around an envelope in which the light source is located [8, 13, 14]. But these systems have many drawbacks, such as low absorption of the visible spectrum, scattering of light from the reaction environment, and reduced processing capacity by mass transfer restrictions. TiO_2 is the most widely used photocatalyst because of its physicochemical properties [8, 9, 15]. In photocatalysis TiO_2 was used in different forms such as nanoparticles suspension [16], nanotubes [17] and film/nanoparticles deposited onto different substrates [9,

18, 19]. The advantage of supporting nanoparticles on substrates is that it eliminates the need to separate catalyst particles from solution after treatment [20, 24-30].

In conventional configurations such as the case of reactors with external lighting, part of the radiation can be absorbed by the support, reducing the efficiency of the catalyst. Lighting with an external lamp represents an obstacle in the design of the compact reactor, due to the size and rigidity of the lamp, high energy consumption and the heat production [11]. The new reactor design presented in this study (with optical fibers as the photocatalyst support) have been developed to overcome these issues. These reactors improve the contact between the catalyst, the light and the pollutant in liquid phase [30]. the idea of depositing the catalyst directly on the surface of the light source is makes possible the design of compact reactors reducing the material transfer limitation by reducing the thickness of air to be treated.

Optical fiber (OF) is composed of a core, which guides the light, and a covering layer [21-25]. The two components have a distinct refractive index so that light can be spread from one end to the other [26, 27]. Textile fabrics used in this study include optical fibers that allow both to transport light within their structure, as well as to emit light laterally within the luminous plastic fiber complex able to diffusely illuminate the whole surface. The optical fibers are distributed to ensure uniform side emitting light throughout the fabric. This maximizes the contact with the photocatalyst (TiO_2) which is directly deposited on the surface of the textile and allows a better distribution of the photons [28, 29]. Several studies of optical fiber coated with TiO_2 have studied the impact of fiber diameter and thickness of TiO_2 layer [8].

The aim of our study is to evaluate the efficiency of heterogeneous photocatalysis processes for hospitals indoor air treatment using a continuous planar reactor at pilot scale and high flowrates. The use of a planar reactor is intended to evaluate the VOC photodegradation limitation step. The novelty of this study is the use a specific textile fiber technology for the VOCs photodegradation in a binary mixture system. With this new configuration, it is possible to obtain a new and compact process without needing external light source. In addition,

following the Langmuir-Hinshelwood and mass transfer model, a design equation was suggested. It can be an excellent basis for the scaling of photoreactor. Our work aims to study the chloroform and glutaraldehyde removal by photocatalysis in a planar reactor at pilot scale. The impact of some parameters, such as the number of optical fiber/LED couples, the inlet concentrations, air flow rate, and relative humidity, on the photodegradation process, is studied. Then, some modeling of the experimental results are provided.

2. Experimental

2.1. Target compounds

In this study, we used two compounds, chloroform ($CHCl_3$) and glutaraldehyde ($C_5H_8O_2$), coming mainly from the hospital sector. Chloroform (99.4% purity) was supplied from VWR BDH Prolab, and Glutaraldehyde 25% in aqueous solution was purchased from Sigma Aldrich.

2.2. Luminous textiles

The optical fibers are the combination of textile fibers (polyester, Trévira CS TM fibres) and plastic optical fibers (POFs) (polymethyl methacrylate). POFs have some advantages over glass /quartz optical fibers; they are less expensive, resilient, flexible [30]. The composite fiber (plastic optical fiber + textile fiber) is made of a POF fiber around which textile fibers are coiled (Fig. 1) [30]. The OFs have a mean diameter of about 500 µm. In fact, the OF core is formed by polymethylmethacrylate resin with an average diameter of 480 µm and covered with 10 µm thick fluoropolymer [8]. For one textile sample, all POFs are collected to one extremity in aluminum connector. The tissue is protected by an intermediate layer of silica, which protects the degradation of the optical fiber by photocatalysis.

The used photocatalyst is the TiO_2 Degussa P25. The textile fiber is soaked for 60 min in a stirred TiO_2 suspension containing of a TiO_2 powder (50 $g.L^{-1}$) and then dried for 2 h at 70 °C. At the end of this process 12 g/m^2 of TiO_2 is uniformly spread on the textile fiber. A single/bi-sided support was supplied by Brochier technologies [30].

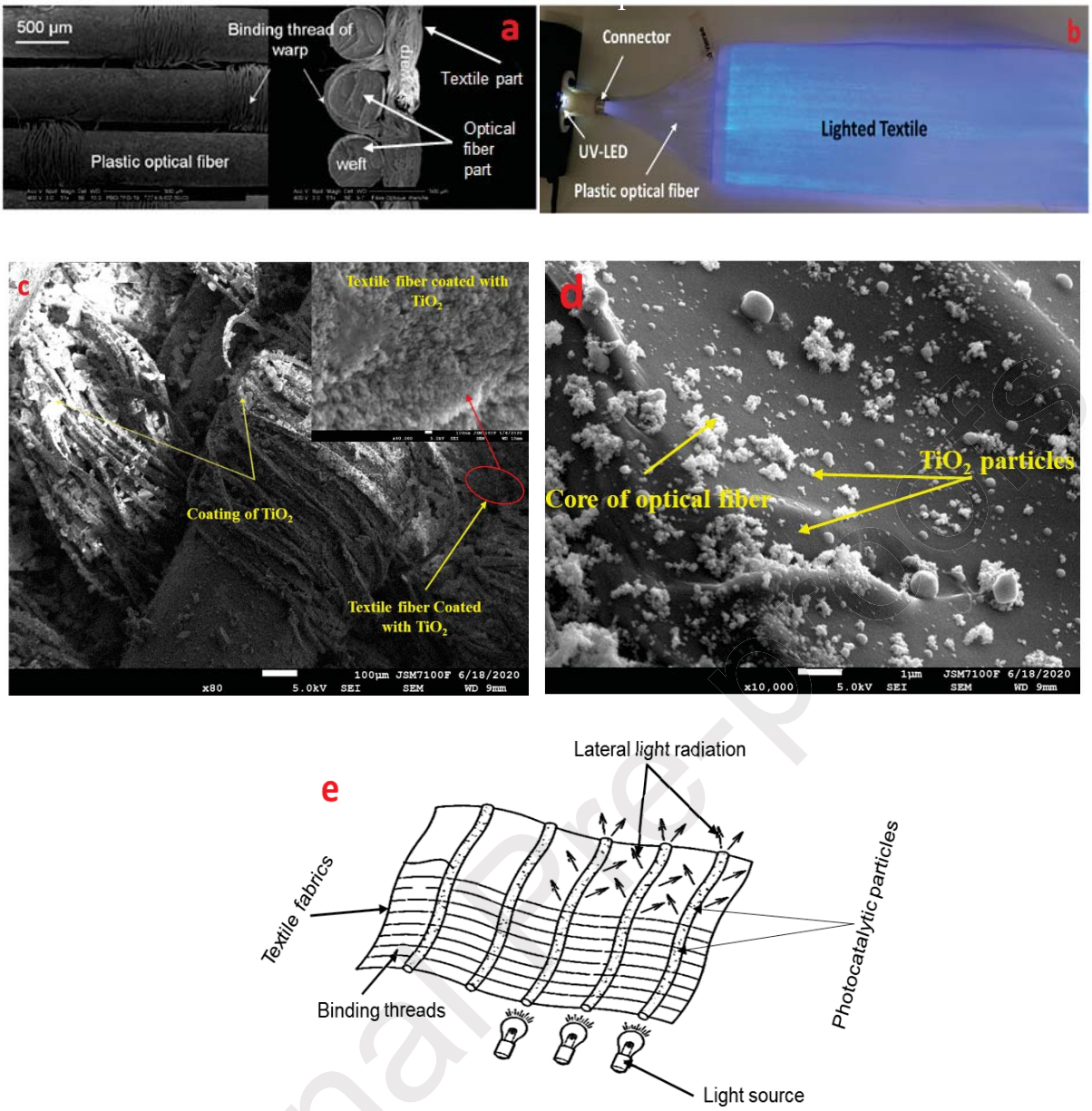

Figure 1. SEM pictures of textile fiber treated: (a) without TiO_2, (b) photocatalytic material, (c), (d) with TiO_2, (d) and (e) are the lighted optical fiber sample and approximate diagram of the optical fiber, respectively.

Figure 1.a shows Scanning Electron Microscopy (using a JEOL JSM 7100 F microscope) of virgin optical fibers with surface treatment for good lateral light emission. Figure 1 (c and d) exhibits optical fibers on which a TiO_2 nanoparticles were deposited (inset of Fig. 1.c). The element of optical fiber is knitted, using the Jacquard process, i.e. the interlacing, in the same plane, of fibers placed in the textile fiber direction (chain), and certain fibers that are placed

perpendicularly to the chain fibers, in the weft direction (the direction of optical fibers) (fig. 1 (a, and c). These Optical fibers are treated to transmit and emit light laterally on their external surface. As shown in figure 1.c, a coating layer of TiO_2 is present on the textile fiber and the beginning threads. Therefore, it makes it possible to activate a large amount of TiO_2, which improves the photocatalytic efficiency.

2.3 Reactor design and setup details

The used photocatalytic reactor consists of a 1 m long rectangular glass chamber having a square section (145 x 145) mm (Figure 2). In order to fix the catalyst, the glass chamber is equipped with glass plates having a length and a thickness of 800 mm and 1 mm, respectively. The distance between the two glass plates can be modified to study its effect on the photocatalytic performance of the reactor. To ensure a good distribution of the radiation on the surface of the catalyst, the optical fibers are supplied with UVA-LED light (wavelength 365 nm and light intensity on optical fiber fabric is around 3 $W.m^{-2}$ before TiO_2 coating and 1.5 $W.m^{-2}$ after coating[)]. The process operates in tangential flow and in a single pass. Before starting the photocatalytic process, the photoreactor (the glass chamber + the photocatalyst) is cleansed with air (12 $m^3.h^{-1}$) under UV light (UVA-LED) for 2 hours to eliminate contamination. The pollutants (VOCs) are injected continuously in the liquid state from a syringe pump system (Kd Scientific Model 100, USA) and introduced into the reactor in the form of a gas flow. A heating tape has been wound around the channel at the level of the injection zone to ensure good evaporation of the pollutants. For each pollutant, a syringe pump system is used. A static mixture ensures the homogenization of the air flow and of the chloroform / glutaraldehyde complex mixture. To maintain the stability of the air flow inlet, a set of valves and a flowmeter (Bronkhorst In-Flow, France) were introduced at the reactor inlet (figure 2.c). The flow rate was varied from 4 $m^3.h^{-1}$ to 12 $m^3.h^{-1}$ (table 1). The air quality (humidity and temperature) was monitored by a specific sensor (Testo 445, Mönchaltorf, Switzerland). In this study, a column

humidifier was used to have dry and humid air with relative humidity (RH) values of 5%, 60 ± 5% and 90%. The different experimental conditions are summarized in Table 1.

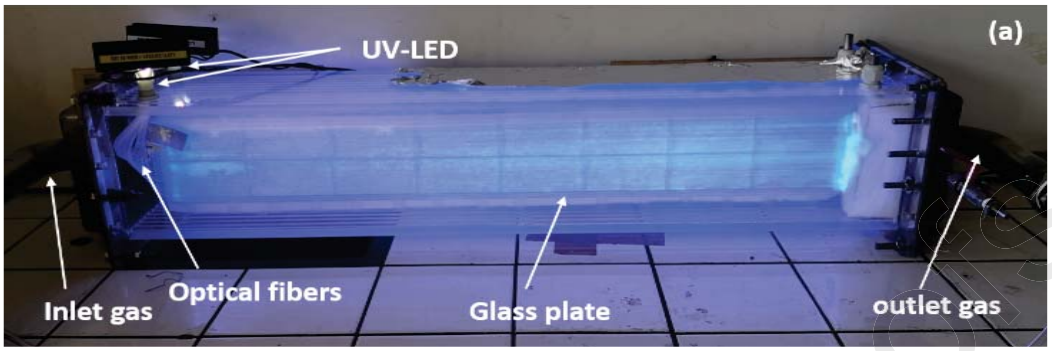

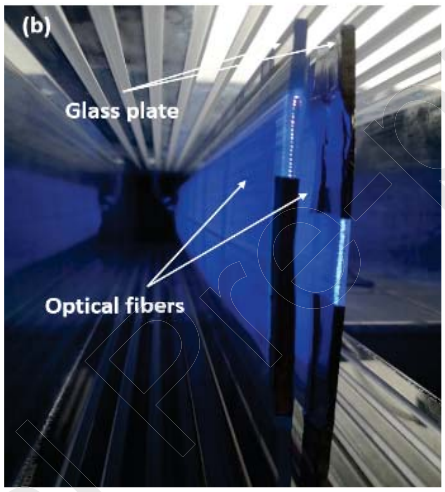

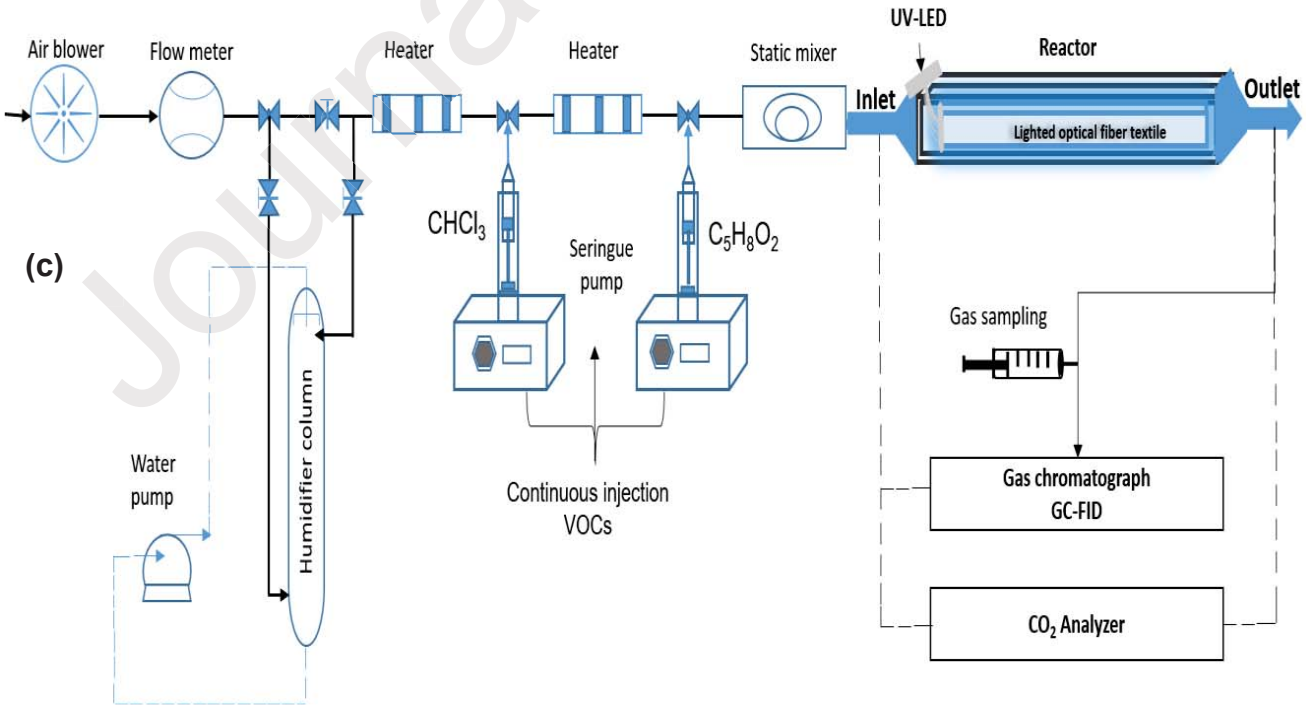

Figure 2. Schematic illustration of the used set-up for VOCs degradation via a new continuous photocatalytic reactor: (a & b) photographic image of the photocatalytic reactor and its internal structure, and (c) the whole experimental set-up.

Table 1. The experimental conditions

Parameter	Value	Unit
Inlet concentration	0.0335, 0.0921, 0.1507, 0.2094, 0.335	$mmol.m^{-3}$
Relative humidity (RH)	5, 60, 90	%
Flow rate (Q)	4, 8, 12	$m^3.h^{-1}$
Light intensity	1.5	$W.m^{-2}$
temperature	20 ±3	°C
TiO_2 concentration	12	$g.m^{-2}$
Optical fiber diameter	500	µm

2.4 Apparatus and analysis

Chloroform and Glutaraldehyde were manually recuperated with a syringe of 500 µL. The inlet/outlet concentrations were measured via a Clarus GC-500 chromatograph equipped with a 60 m **x** 0.25 mm polar DB-MS capillary column (film thickness: 0.25 µm). The GC chromatograph is equipped with a flame ionization detector (GC-FID). The FID is powered by a mixture of air and hydrogen (H_2). The Helium gas (He) was used as a vector gas at a flow rate of 1 $ml.min^{-1}$. The injection and detection temperatures were both kept at 250 °C. The oven temperature was initially maintained at 50 °C for 3 min, then programmed to increase to 100 °C (2°C/min), reaching maximum temperature after 10 min. The CO_2 analyzer is a MIR 9000 Environment SA multi-gas infrared analyzer equipped with GFC (Gas Filters Correlation) technology. The CO_2 amount formed during the photocatalytic process was measured by a Fourier Transform Infrared (FTIR) spectrophotometer brand Environment SA.

3. Results and discussion

To evaluate the performance of the process, i.e. the removal efficiency (RE) and the selectivity to carbon dioxide (SCO_2), we use the following equations (1) and (2):

$$\mathrm{RE}\ (\%) = \frac{[\mathrm{C}]_{\mathrm{inlet}} - [\mathrm{C}]_{\mathrm{outlet}}}{[\mathrm{C}]_{\mathrm{inlet}}} \mathrm{x}100 \qquad (1)$$

where $[C]_{inlet}$ and $[C]_{outlet}$ are the inlet and the outlet concentrations of the pollutants ($mg.m^{-3}$), respectively.

Selectivity of CO_2: $$SCO_2(\%) = \frac{[\mathbf{CO_2}]_{\mathbf{outlet}} - [\mathbf{CO_2}]_{\mathbf{inlet}}}{n_{c,voc}\mathrm{xRE}(\%)\mathrm{x}[\boldsymbol{VOC}]_{\mathbf{inlet}}} 10^4 \qquad (2)$$

where $n_{c,VOC}$ and [VOC] are the number of carbon in the molecule of the pollutant and the inlet concentration of VOC, respectively.

This study aimed to treat a mixture of VOCs of different natures. To understand the oxidative behavior of these pollutants in the mixtures, the analyses were carried out on each composite alone. Before starting the analysis of pollutants, the air flow in the reactor must reach equilibrium. It is necessary to wait a few minutes after the pollutants have been injected into the air flow through the reactor in order to stabilize their concentrations.

3.1.1. Study of mono-compound system (Case of Chloroform ($CHCl_3$)

Effect of inlet concentration and flow rate on photocatalytic process

The photocatalytic degradation of chloroform was examined in the planar reactor under various inlet concentrations and flow rates. The inlet concentration of chloroform was varied from 4 $mg.m^{-3}$ to 40 $mg.m^{-3}$ for different flow rates, i.e., 4, 8, and 12 $m^3.h^{-1}$. The results of the removal efficiency of chloroform at different inlet concentrations and different flow rates are shown in figure 3.

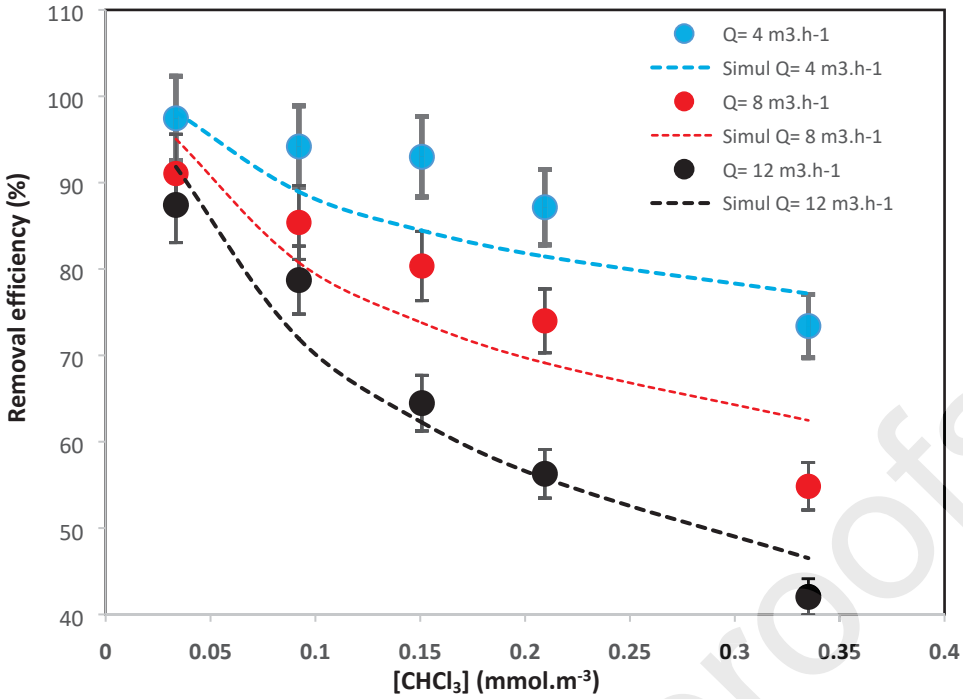

Figure 3. Removal efficiency (RE) of chloroform with different inlet concentration at different flow rates, (LED- UV intensity = 1.5 W.m^{-2}, relative humidity (RH) = 60 ± 5%).

It is observed (Fig. 3) that at constant air flow, the removal efficiency decreases as the initial inlet concentration of the pollutant increases. In fact, the greater the air flow, the less time the pollutant will have to be adsorbed in sufficient quantity on active sites located on the surface of the catalyst [31-34]. In addition, the removal efficiency clearly decreases as the air flow increases; this can be explained by the reduction in the contact time between the polluting molecules with the active sites on the surface of the catalyst [22, 35-38]. This means that a reduced amount of chloroform is able to react with reactive species such as $OH^{\cdot}$ and $O_2^{\cdot}$ produced on the catalyst surface. Similar results have been reported for the removal of chloroform [11], butyraldehyde and ammonia [30], and isovaleraldehyde [34] using a glass fiber tissue with an external UV lamp in a cylindrical reactor. Moreover, the removal capacity of 25 mg.m^{-3} of chloroform through the optical fiber (with 12 g/m^2 of TiO_2) is about 81.812

mg/h.g_{TiO2}, while the removal capacity of the same concentration through the glass fiber tissue (with 13 g/m^2 of TiO_2) [11] is about 18.846 mg/h.g_{TiO2}.

Effect of inlet concentration and water vapor on the photocatalytic oxidation

Many studies reported that the relative humidity (RH) could considerably affect the trend of gas-phase photocatalytic reaction [29-31, 35-39]. In this context, the impact of relative humidity on the degradation of VOCs was investigated by applying different relative humidity values (5, 60, and 90%). Figure 4 shows that an increase in the inlet concentration of chloroform increases the degradation rate at low relative humidity (5% - 60%); hence, water molecules have a significant effect on the degradation rate of chloroform. For an inlet concentration of 0.0335 mmol.m^{-3} (Fig. 4) the degradation rate increases from 0.88 µmol.m^{-2}.s^{-1} to 1.52 µmol.m^{-2}.s^{-1} as RH increases from 5% to 60%.

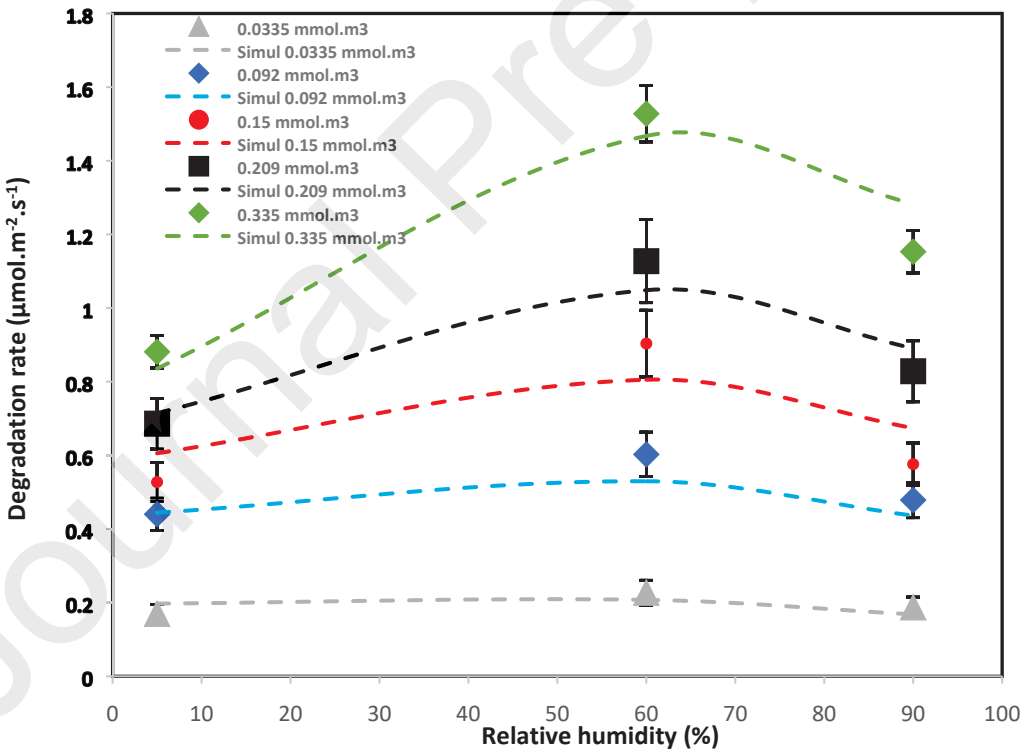

Figure 4. Effect of the relative humidity on the photocatalytic removal of Chloroform, (T=20°C, Q= 4m^3.h^{-1}).

In most cases, water molecules are at the origin of the formation of $OH^{\cdot}$ radicals [41, 46]. Therefore, a slight increase in relative humidity (i.e. water molecules) enhances the photogeneration of $OH^{\cdot}$ radicals (as a very active species) [43, 44], and leads to additional adsorption of the pollutant and an increase in the kinetics of photocatalytic elimination. When the humidity increase (above RH = 60%), the competitive effect between H_2O and $CHCl_3$ molecules on active sites becomes greater and results in a decrease in the degradation rate. In addition, water molecules can bind to hydroxyl radicals on the surface of the catalyst and to each other via its hydrogen bond, forming highly organized layers [46], which act as a physical barrier that reduces forces between Chloroform and the photocatalyst surface. Considering the big difference between water vapor and chloroform and the fact that most chloroform molecules adsorb to the surface of the catalyst via Van Der Walls interactions, which are much weaker than hydrogen bonding of water, the adsorption of water dominates that of chloroform in [46]. Besides the photocatalytic process, relative humidity level can greatly affect the type and the quantity of by-products [47]. Abou Saoud et al [33] obtained similar results when they studied the effect of relative humidity on the ammonia and butyraldehyde degradation, and discovered that the presence of water molecules improves the degradation rate of butyraldehyde at an average humidity value around 50-60%. Zadi et al [11] studied the photocatalytic degradation of chloroform in a cylindrical TiO_2/GFT-based reactor with conventional lighting, and obtained almost 70% of RE for 25 $mg.m^{-3}$ inlet concentration. Assadi et al studied the effect of RH on the photocatalytic degradation of isovaleric acid and reported that, at medium relative humidity, the photocatalytic oxidation can reach a maximum compared to dry air and to high RH [34]. Therefore, on one hand, the total absence of H_2O molecules is deadly for the photocatalytic process, as it affects the amount of hydroxyl radicals formed on the catalyst surface. On the other hand, a high-water concentration can negatively affect the photocatalytic degradation of the VOC pollutant due to the competition between H_2O and VOC

molecules [43]. Table 2 summarizes some works that investigated the impact of some operating parameters on the efficiency of VOCs removal.

Table 2. Comparison of some results obtained in the literature with external UV lamp.

Authors	catalysts	VOCs	Studied parameters	Optimal results
Mamaghani et al [51]	commercial TiO_2 photocatalysts	Toluene, methyl ethyl ketone	$[VOC]_{inlet}$ and Q RH	Q= 6 $L.min^{-1}$ RH= 20%
Zhang et al [43]	TiO_2/diatomite	Formaldehyde, acetone, and p-xylene	$[VOC]_{inlet}$ and Q RH	[VOC]= 10 ppm Q= 1 $L.min^{-1}$ RH= 0%
Abou Saoud et al [32]	Glass Fiber Tissue (GFT)	butyraldehyde (BUTY), dimethyl disulfide (DMDS)	$[VOC]_{inlet}$ and Q	Q= 4 $m^3.h^{-1}$
Zadi et al [31]	SiO_2-TiO_2 coating on the fiber glass Tissue (GFT)	propionic acid (PPA), and benzene (BENZ)	$[VOC]_{inlet}$ and Q RH	Q= 2 $m^3.h^{-1}$ RH= 50%
Abou Saoud et al [33]	TiO_2 coating on the GFT	Ammonia (NH_3) and butyraldehyde (C_4H_8O)	$[VOC]_{inlet}$ and Q	Q= 1 $m^3.h^{-1}$ RH= 55-60%

Effect of the gap between catalyst plates on chloroform removal

The effect of the space in which the gas flows on the photocatalytic performance is studied by modifying the distance between the two glass plates installed in the reactor and supporting the catalyst. The distance between catalysts' plates can greatly influence the step of mass transfer and hence the removal efficiency. Three positions (0, 2.5, and 5 cm) between catalysts are investigated. Figure 5 shows the effect of catalysts' positions on the photocatalytic

degradation. For an air gap of 2.5 cm, the removal efficiency reaches a maximum of 97% for an inlet concentration of 4 $mg.m^{-3}$. When both catalysts are confused, the catalyst surfaces are reduced so that there will be only one catalyst; this position prevents the diffusion of VOC molecules on all catalyst surfaces, due to the decrease in the active surface of the catalysts. Regardless of the initial inlet concentration, it can be noted that the $CHCl_3$ removal decreases in the case where the separation is 5 cm. This trend can be due to a limitation of mass transfer.

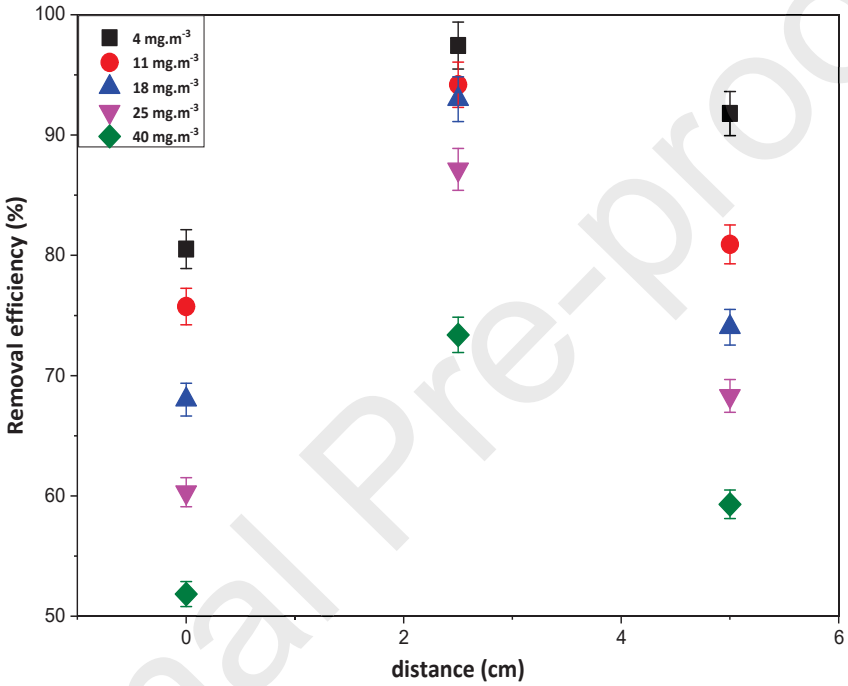

Figure 5. Effect of the distance between both textile catalysts on chloroform removal (T=20°C, Q=4 $m^3.h^{-1}$, RH= 60 ± 5%).

3.1.2. Case of glutaraldehyde ($C_5H_8O_2$)

Hospital indoor air contains a wide range of volatile organic compounds: disinfectants, sterilizers, cleaning products [52]. Thus, in order to evaluate another type of indoor air pollutant in hospitals and after the optimal conditions have been determined, a series of photocatalytic experiments were carried out to degrade glutaraldehyde under these optimal conditions. In

these experiments, the same degradation profile as chloroform was obtained with a slightly higher removal efficiency (Fig. 6). Therefore, it can be noted that the variation of the inlet concentrations and the flowrates have an influence on the removal efficiency, regardless of the pollutant. According to figure 6, and at a flowrate of 12 $m^3.h^{-1}$, the RE is 88% and 65% for an inlet concentration of 0.0335 $mmol.m^{-3}$ and 0.335 $mmol.m^{-3}$ respectively. While for chloroform, it is about 87% and 42%, respectively. This difference in RE may be due to the chemical properties of each of the organic compound, such as molar weight and compound's affinity.

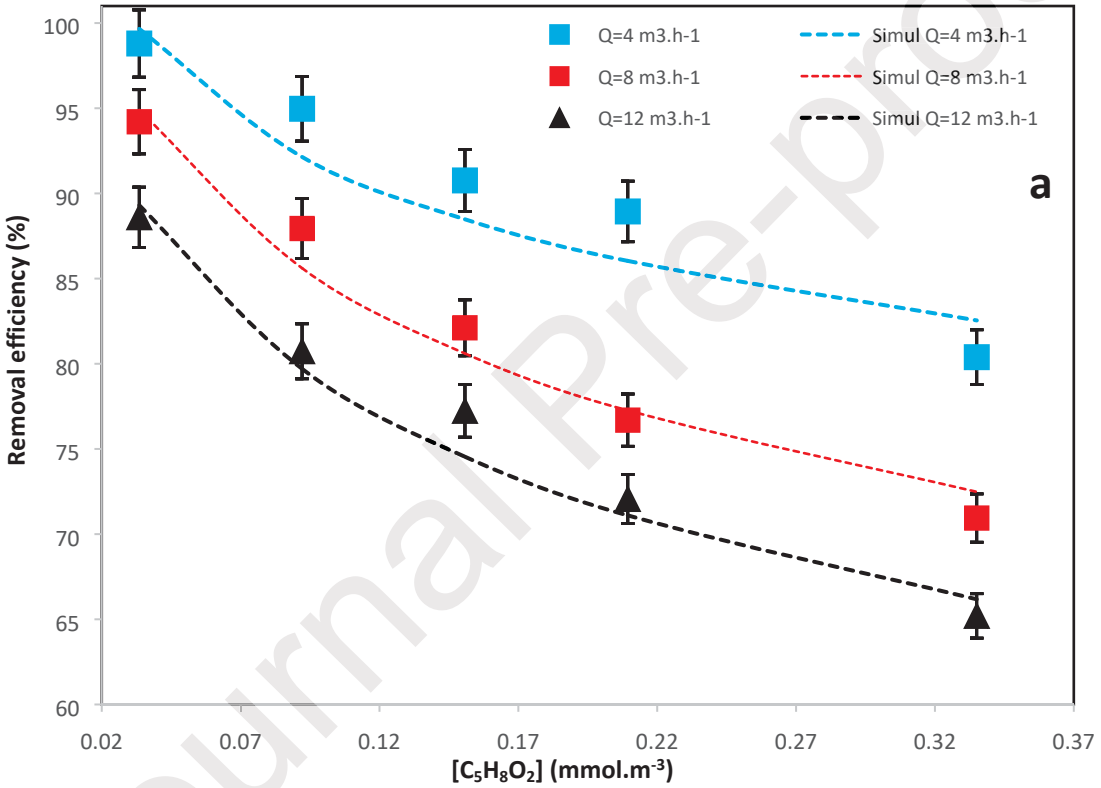

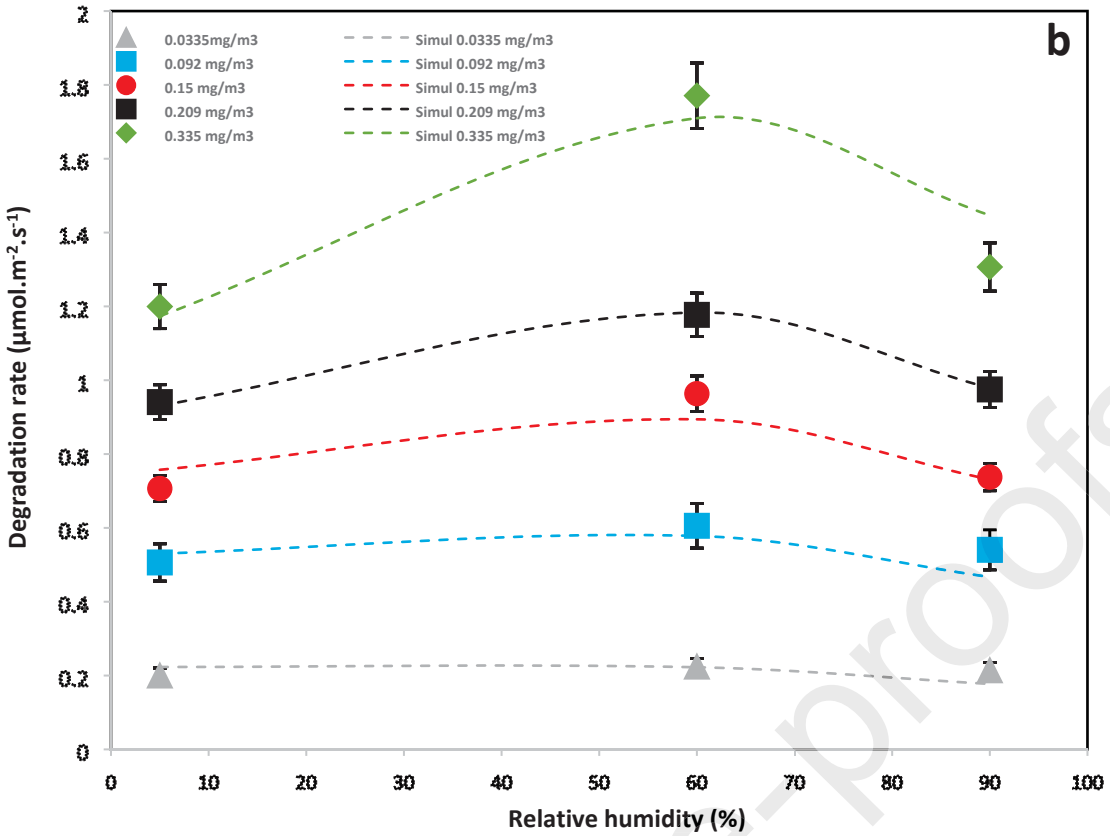

Figure 6. Removal efficiency (RE) of glutaraldehyde with different inlet concentration at different flow rates and at average humidity (RH) = 60 ± 5%) (a), and Impact of the relative humidity on its degradation rate with different inlet concentration at different relative humidity values and at Q= 4$m^3.h^{-1}$ (b). (T=20°C, LED- UV intensity = 1.5 $W.m^{-2}$).

Results observed in Fig.6-b confirm that the degradation rate is influenced by the relative humidity Levels. In addition, the highest removal rate was obtained under average humidity conditions (same results than for Chloroform; Fig. 4). From these results, it is worth noting that the maximum degradation rate was obtained at the rage between 45-65% of RH for both pollutants. The degradation rate decreases at high RH levels, which could be due to competition between adsorbed VOC and H_2O molecules. Zhang et al [50] suggested that, at an average relative humidity level (15% -25%), it is possible that water molecules are physisorbed as hydroxyl groups on the surface of the catalyst via hydrogen bonding; these hydrogen bonds form one or more layers, which inhibit the arrival or delay the contact of the

pollutant with the reactive surface of the catalyst or with the radical species in the boundary layer.

3.1.3. Photocatalytic degradation of VOCs in binary mixture system ($CHCl_3/C_5H_8O_2$) and its effect on CO_2 formation

The purpose of this part is to compare the RE of chloroform ($CHCl_3$) and glutaraldehyde ($C_5H_8O_2$) treated separately, with their degradation rate when they are mixed. An equimolar mixture of chloroform and glutaraldehyde was injected into the incoming air. The experiments were carried out at different inlet concentrations of VOCs under a flow rate of 4 $m^3.h^{-1}$, 20°C, and 60% RH. The distance between both photocatalysts was maintained at 2,5 cm. Figure 7.a shows that the removal efficiency of chloroform and glutaraldehyde in the mixture ($CHCl_3/C_5H_8O_2$) is lower than that of the pure compound. Hence, the VOC removal kinetics shows a global slowdown in the case of binary mixture. For example, in the case of chloroform, this slowdown could be partly attributed to the involvement of other primary and / or intermediate VOCs in the consumption of species containing chlorine [43]. The same behavior was observed by Debono et al [49] when they studied the ternary mixture of toluene, decane and trichloroethylene (TCE); they connected the slowdown of the removal kinetics of TCE to the participation of chlorine-containing species in the degradation of other primary and/or intermediate VOCs in the reaction (i.e., the consumption of chlorine containing species by other VOCs). In general, in the case of a binary mixture of VOCs, the decrease in removal efficiency is based on the competitive adsorption between the two compounds to access the surface of the catalyst [31, 33, 44]. Studies by Chen et al [50] have already reported the inhibitory effect of a ternary mixture of VOCs using equimolar concentrations of toluene, ethanethiol and ethyl acetate; they also related the effect of the mixture on the VOCs elimination with the respective adsorption capacities of the VOCs on the photocatalyst surface. In our work, we noticed that $CHCl_3$ is the more volatile compound ($P_{sat.vapor}$ = 21.2 kPa at 20

°C) and more affected by the competition effect than the $C_5H_8O_2$ ($P_{st.vapor}$= 2.3 kPa at 20 °C). As a result, the photocatalytic degradation of $CHCl_3$/$C_5H_8O_2$ in a binary mixing system also has an influence on CO_2 formation during the photocatalytic process. Figure 7.b shows the carbon dioxide (CO_2) selectivity during the photocatalytic oxidation of Chloroform and glutaraldehyde in a simple or binary mixture system.

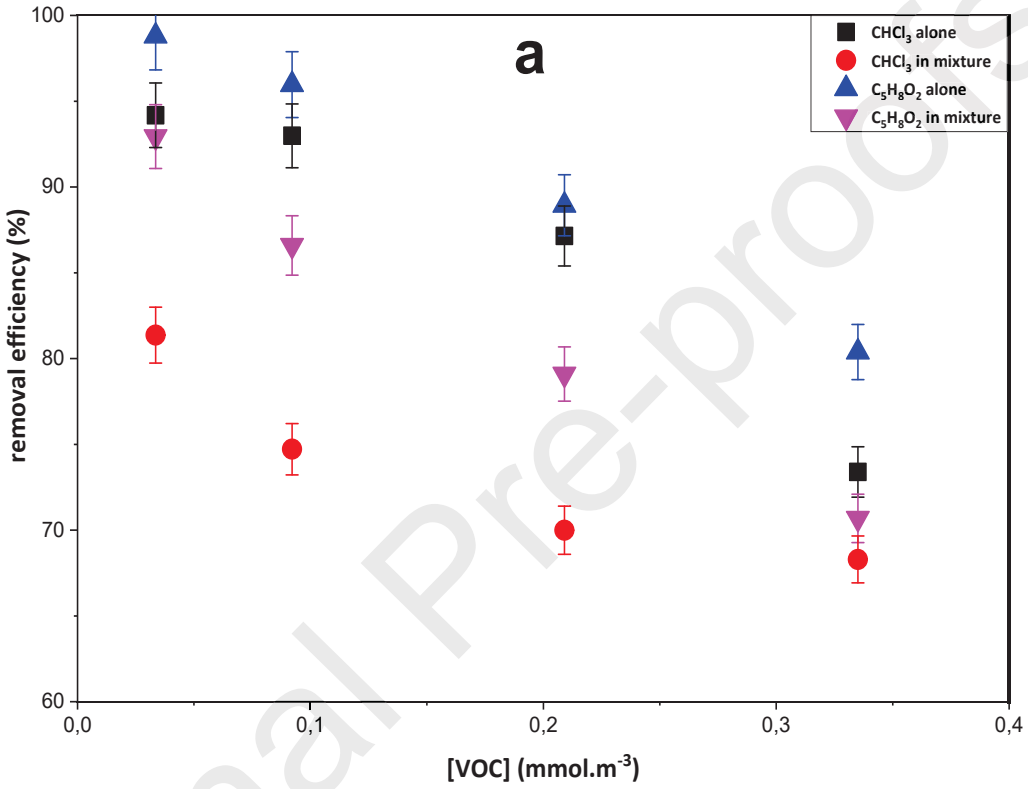

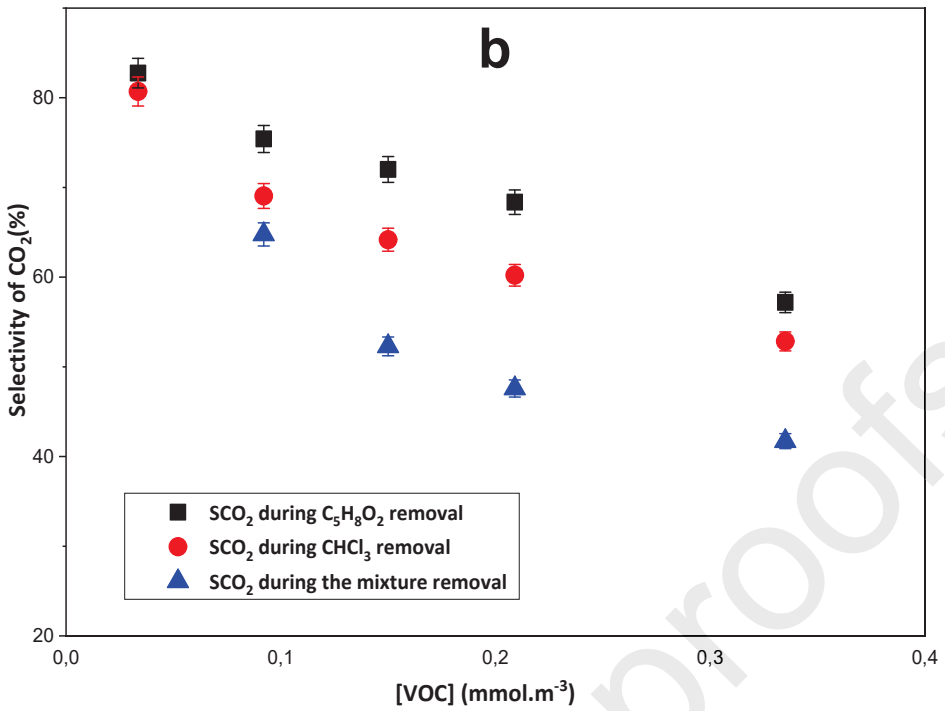

Figure 7. (a) Effect of mixture on the photocatalytic removal of chloroform and glutaraldehyde and (b) on the CO_2 formation during the photocatalytic process,

(T=20°C, Q=4 $m^3.h^{-1}$, RH= 60 ± 5%).

Carbon dioxide (CO_2) is the predominant by-product. An increase in the initial concentration of VOCs leads to a significant decrease in the selectivity to CO_2. For large concentrations of pollutants, the number of reactive photo-generated species saturates. Chloroform and glutaraldehyde are only mineralized in a small fraction, which corresponds to the formation of CO_2. The improvement in CO_2 selectivity is clearly noticeable at low concentrations; at low input concentrations, there is more availability of active sites, so the intermediate by-products can be more easily degraded to the final CO_2 stage. Therefore, a competition phenomenon appears between glutaraldehyde, chloroform, and their by-products. This competition depends on the respective concentrations of each chemical entity and the compounds' affinity with the catalytic support [31, 33, 54-56]. It can be seen in Figure 7.b that CO_2 selectivity decreases

during the degradation experiment of the binary system; this could be due to the competition effect between VOCs and their by-products.

3.1.4. Effect of the number of optical fiber fabric/LED with optimal air gap

To further improve chloroform degradation, at optimal distance between sheets (d =2.5 cm) different combinations using one or more Optical fibers fabric/LED couples (OF/UV-LED, 2OF/2UV-LED, and 3OF/3UV-LED) have been installed in a parallel configuration into the reactor, as shown in Figure 2. The chloroform removal profile as a function of the number of PS/LED couples, at different inlet concentration ranging from 4 $mg.m^{-3}$ to 40 $mg.m^{-3}$, is shown in figure 8. Each photocatalytic sheet has an active area of 800 cm^2, which increases linearly to reach 1600 cm^2 or 2400 cm^2 for 2 or 3 sheets. The distance between the catalysts is always 2.5 cm. It is readily seen that the oxidation performance of chloroform increases as a function of the number of photocatalyst sheet/UV-LED couples. However, for low concentrations (4 $mg.m^{-3}$), it can be noted that the removal efficiency of chloroform is almost the same for all three cases (1, 2, and 3OF/UV-LED), i.e. about 96% on average. This behavior can be due to the higher availability of active sites on the photocatalyst surfaces, for the three cases. It was found that the removal efficiency of chloroform is about twice greater for 3OF/UV-LED than for a 1OF/UV-LED. This can be explained by the increase in the number of active surfaces due to the increase of the TiO_2 surface area and then the number of reactive species ($OH^{\bullet}$, $O_2^{\bullet}$, …), and to the increasing number of photons emitted in the system. This means that if we need more reactor efficiency, we can increase the number of PS/UV-LED couples. Similar results were obtained by Tugaoen et al [24] when they treated the water using optical fiber immobilized TiO_2 reactor.

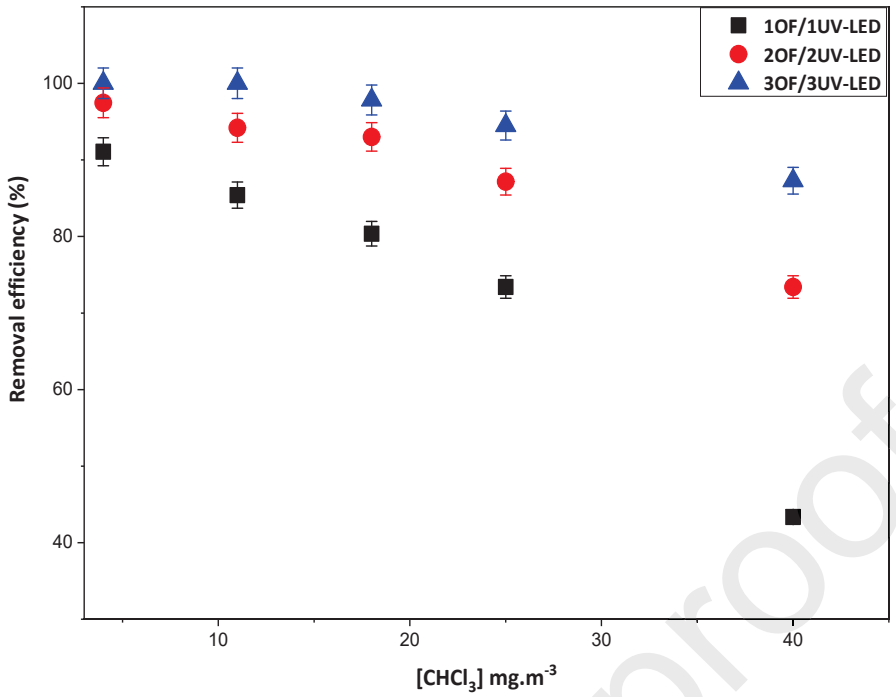

Figure 8. Impact of the number of OF/UV-LED couples on the removal efficiency of Chloroform at different inlet concentrations. (Q= 4$m^3.h^{-1}$, RH= 60 ± 5%, T=20 °C).

3.2. Kinetic modeling of the degradation with contribution of mass transfer on the planar reactor

For most catalytic gas-solid reactions, as well as heterogeneous photocatalysis, the Langmuir Hinshelwood (L-H) rate form was used [33, 41, 55, 58]. The L-H rate equation has been widely recognized as providing good correlations for heterogeneous reactions. In this way, some calculations were made to evaluate mass transfer's role. These calculations were performed using different gas flow rates and different concentrations in order to study the effect of the external mass transfer between the bulk fluid and the outer surface of the thin film catalyst. The expression of L-H rate has been widely employed in the literature [34], [57-59] to describe the photocatalytic reaction on the surface of the catalyst. Generally, two main steps in the photocatalytic process can be considered, the mass transfer step and the chemical reaction step. Based on the results obtained on the effect of the air gap on the removal efficiency, it is

necessary to consider the mass transfer step. In this study, the used photocatalytic reactor presents a negligible resistance to the intraparticle transport as a result of the non-porous configuration of thin-film catalyst. Therefore, in this case, just the mass transfer between the catalyst and the bulk fluid can be considered [34, 59, 60]. As the photocatalysis process involves reactive surface sites, it seems consistent that internal diffusion is negligible, whether Knudsen or molecular [41, 59, 60]. Thus, in the mass transfer model, only the impact of external mass transfer in the apparent degradation rate for equations (3) and (4) is considered. The kinetics of VOC photocatalysis have been formulated by many authors [55, 61, 62] following (eq. (3) and (4)):

In the gaseous phase:

$$u\frac{dC^m}{dz} + k_m a_v(C^m - C^s) = 0 \qquad (3)$$

In the solid phase:

$$k_m a_v(C^m - C^s) = k_{obs}\frac{K_m C^s}{1 + K_m C^s} \qquad (4)$$

Where, u and k_{obs} are the flow velocity of the gas (m.s^{-1}) and the observed kinetic constant. The bulk and surface concentration are referred to as C^m and C^s, respectively. K is the adsorption constant, ***m*** and ***n*** indicate the pollutant and by-products, respectively, and a_v is the medium area per unit volume of the reactor ($m_{TiO2}^2/m_{reactor}^3$). The chloroform and glutaraldehyde concentrations at inlet are very low, so the amount of their by-products formed would also be very low and their competitive effect will be neglected [34, 55, 63]. The global mass balances of the different phases are necessary in the continuous flow reactor [59, 64]. For mass transfer calculations, the viscosity and density of the fluid are assumed to be similar to that of air. The Reynolds number at flowrates ranging from 4 - 12 m^3.h^{-1}, corresponds to 492.62 - 1477.86, respectively. Thus, the flow regime into the reactor is laminar (Re < 2000) [65]. For this reason, it was suggested that the mass transfer stage can be considered. The coefficient of external mass transfer, $\boldsymbol{k_m}$, is function of the flow regime of the fluid and the

nature of the gas phase. It can be established using a semi-empirical correlation (eq.5) [34, 67]:

$$Sh = 0.664(\mathrm{Re})^{(\frac{1}{2})}.(\mathrm{SC})^{(\frac{1}{3})} \quad \text{For} \quad \mathrm{Re}<10^5 \tag{5}$$

Where Sh, Re and Sc are the dimensionless numbers of Sherwood, Reynolds and Schmidt, respectively. The molecular diffusivity ($\boldsymbol{D_m}$) of the pollutants is calculated using the Fuller, Schettler and Giddings correlation (eq.6) [62]:

$$D_m = \frac{10^{-3}T^{1.75}}{P\left[(\sum v)_A^{(\frac{1}{3})} + (\sum v)_B^{(\frac{1}{3})}\right]^2}\left(\frac{1}{M_A} + \frac{1}{M_B}\right)^{(\frac{1}{2})} \tag{6}$$

Where T, P are the absolute temperature (K) and the pressure of the gas stream (Pa), respectively. $(\sum v)_A$, $(\sum v)_B$, M_A, M_B are the atomic volumes of diffused air (A) and pollutant (B), obtained as the summation of the atomic values of individual atoms that compose the molecular structure of species (A) and (B), and the molecular weights of A and B ($g.mol^{-1}$), respectively. With equation (6), we can evaluate the diffusivity coefficients of the pollutants, and then the mass transfer coefficients. Table 3 presents the diffusivity values of Chloroform and glutaraldehyde in air.

Table 3: Diffusivity values of Chloroform and glutaraldehyde in air

Pollutants	Formula	Diffusivity in the air D_m (cm^2/s)
Chloroform	$CHCl_3$	0.0884
Glutaraldehyde	$C_5H_8O_2$	0.0778

The mass transfer coefficient values ($\boldsymbol{k_m}$) can be deduced from the relationship between eq.6 and the links of the diffusion coefficient $\boldsymbol{D_m}$ and the Sherwood number (eq. 7):

$$N_{sh} = \frac{k_m d}{D_m} \tag{7}$$

Where, ***d*** is the equivalent diameter.

Table 4 shows the Reynolds number and mass transfer coefficients in the planar reactor.

Table 4: Reynolds number and mass transfer coefficients

Flowrate (Q, $m^3.h^{-1}$)	**Reynolds number**	**Mass transfer coefficient ($k_m \times 10^3$, $m.s^{-1}$)**	
		Chloroform	Glutaraldehyde
4	492.62	5.0395	4.6282
8	985.25	7.1270	6.5453
12	1477.86	8.7287	8.0163

After k_m coefficients have been calculated, kinetics are generally considered as a first-order type to consider $KC^s<1$ to simplify eq. (3) and (4) [41]. However, the Maple software is used to approach the solution of the non-simplified system according to the series method. Also, second-order development has been shown to be sufficiently accurate due to our analytical equipment and the high precision assessment, in the order or less than 5%, from second to third order approaches has been observed [34, 65].

The second order development is:

$$C_{in} - C_{out} = \frac{Lk_m a_v}{2u}\left[C_{in} + \frac{1}{K} + \frac{k_{obs}}{k_m a_v} - \sqrt{\left(-C_{in} + \frac{1}{K} + \frac{k_{obs}}{k_m a_v}\right)^2 + \frac{4C_{in}}{K}}\right] \quad (8)$$

In this 2nd order development (eq. 8), k_{obs} and K are the two unknown parameters. Both are determined by the numerical simulation with Excel solver [41, 59]. We define a target cell for each experimental point as the difference between the experimental and theoretical outlet concentration. For each compound, the sum of the square of the target of cells is minimized by the optimization of the two variable cell values. It is therefore possible to find the best k_{obs} and K values for chloroform and glutaraldehyde. This model offers a good description of the experimental results (Fig.4 and fig. 6).

The k_{obs} and K values are summarized in Table 5

Table 5: k_{obs} and K values for Chloroform and glutaraldehyde

VOC	Chloroform	Glutaraldehyde
k_{obs} (mmol.m^{-3}.s^{-1})	0.0425	0.0886
K (m^3.mmol^{-1})	2.7367	1.1585
R^2 (%)	99.89	99.57

In addition, the influence of the flow regime is completely integrated by the parameter k_m. It is therefore interesting to note that these constants do not depend on flowrates. Then, with this L-H model, a separation between the mass transfer and the stage of the chemical reaction were presented. Thereafter, it is possible to use these more reasonable constants (k_{obs}, K) that do not depend on the flow rate to investigate the effect of relative humidity on the degradation rate at each flowrate

3.3. Modeling the impact of the relative humidity on the removal efficiency

For both studied VOCs, it was found that an optimal RH value was obtained (Fig.4 and 6.b). Interestingly, when the inlet concentration increases, more emphasis is placed on this optimal value. This result is probably attributable to the fact that, under these conditions, there is a greater competition effect between water and VOCs. For example, if the number of active sites is constant, it seems evident that the competitiveness increases as the inlet concentration increases. These results are consistent with previous work on the degradation of trimethylamine [54], propionic acid and benzene [31], and cyclohexane [58]. L-H bimolecular model can be used to correlate the experimental data by treating VOC/water system as binary mixture system [41, 67]. The kinetics of degradation can be written as follow (eq.9):

$$r_A = k_{obs} F_A F_W \quad (9)$$

With

$$F_A = \frac{K\mathrm{C_A}}{(1 + \mathrm{KC_A} + \mathrm{K_W C})} \quad (10)$$

And

$$F_W = \frac{\mathrm{K'_W C_W}}{(1 + \mathrm{K'_A C_A} + \mathrm{K'_W C_W})} \quad (11)$$

So eq. (9) is written as:

$$r_A = k_{obs} \frac{K\mathrm{C_A}}{(1 + \mathrm{KC_A} + \mathrm{K_W C})} \frac{\mathrm{K'_W C_W}}{(1 + \mathrm{K'_A C_A} + \mathrm{K'_W C_W})}$$

Where $\mathrm{C_W}$, $\mathrm{K_W}$ are the water vapor concentration and the related Langmuir adsorption constant, respectively. $\mathrm{K'_A}$ and $\mathrm{K'_W}$ are the competitive adsorption constants of pollutant and water, respectively. The constant k_{obs} and K are taken from table 5.

All model constants are solved numerically using the Excel solver. They are presented in Table 6.

Table 6. The values of L-H model of each VOC test

VOC	K_{obs} (mmol.m^{-3}.s^{-1})	K (m^3.mmol^{-1})	K_W (m^3.mmol^{-1})	K'_A (m^3.mmol^{-1})	K'_W (m^3.mmol^{-1})
Chloroform	0.042	2.73	0.0109	1.3097	0.0047
Glutaraldehyde	0.088	1.15	0.014	2.2848	0.0028

As shown in Fig. 4 and Fig. 6.b, the model correlates well with the experimental results. Thus, it is possible to estimate the effect of water vapor on the photodegradation at different pollutant and at different inlet concentrations. The optimal humidity condition for photocatalytic degradation of chloroform and glutaraldehyde are approximately 45-65%.

3.4. TiO_2/optical fiber recyclability

In order to evaluate the stability and reuse of the TiO_2-coated optical fiber (TiO_2/optical fiber) used in this study, repetitive photocatalytic cycles (C_i) were applied, under the same experimental conditions as those of the first cycle, for the chloroform degradation at different Inlet concentrations (4mg.m^{-3} up to 40mg.m^{-3}). After each experiment, the photoreactor is purified with air (12 m^3.h^{-1}) under UV light (UVA-LED) for 2 hours to eliminate all contamination.

So as can be seen in figure 9, the optical fiber has a good stability, approved by the slightly decrease of the degradation efficiency after 4 cycles.

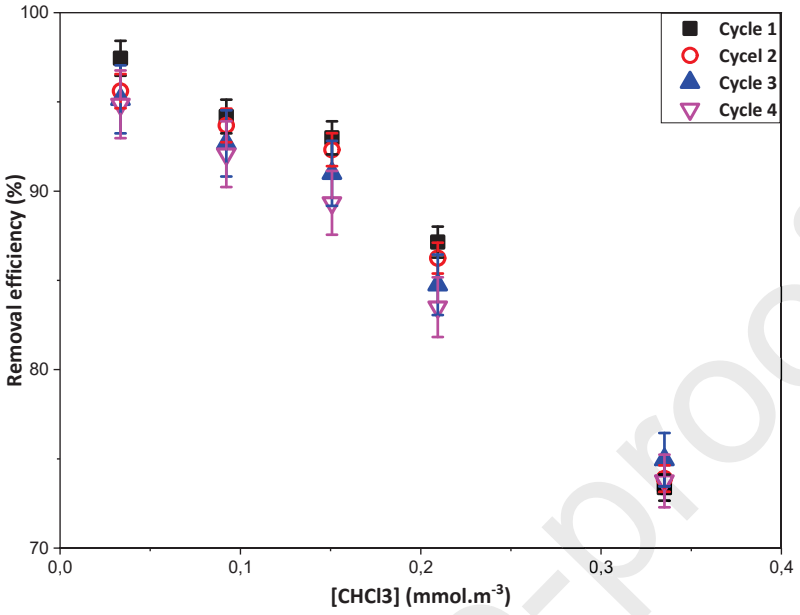

Figure 9. Recycling runs of the TiO_2/optical fiber for the photocatalytic degradation of chloroform at different inlet concentrations (4mg.m^{-3} up to 10 mg.m^{-3}), (T=20°C, Q = 4m^3.h^{-1}, N_{sheet} = 2, RH=60 ± 5%).

To confirm this stability, the reaction rate constant k and the adsorption constant K were determined using the solver Excel (Table 7). According to the later, there is no significant difference between the coefficient values, which allows us to confirm the stability of the catalyst. On the other side, this finding confirm that the reaction does not occurs in the gas phase but on the photocatalyst surface by a Langmuir-Hinshelwood mechanism. In addition, (C1, C2, C3, and C4) in fig. 9 shows the conversion of the inlet concentration of chloroform. We have shown above that the pollutant inlet concentration influences the removal efficiency, but it does not have a significant impact on both constants (kobs, and K). As a result, the photocatalytic oxidation, at this range of chloroform concentration (i.e. low concentrations), is not limited by the number of active sites on the TiO_2/OF photocatalyst, and that there is no

competitive adsorption phenomenon between chloroform and its by-products. In the same context, Bouzaza et al [65] demonstrated that at high concentrations (e.g. ppmv), phenomena of catalyst saturation and adsorption competition are generally observed.

Table 7. K and k_{obs} parameter values of the L-H model for 4 successive cycles.

	Cycle			
	C_1	C_2	C_3	C_4
k_{obs} (mmol.m^{-3}.s^{-1})	0.042	0.043	0.0463	0.0456
K (m^3.mmol^{-1})	2.73	2.614	2.394	2.416

In order to mitigate real hospital lighting, doping can red shift the spectral absorption of TiO_2 leading to VOC removal under actinic indoor light [17, 68-70].

4.Conclusion

This work aims to study the photocatalytic performance of a new system formed from TiO_2 nanoparticles and optical fibers for the degradation of pollutants potentially existing in the indoor air of hospitals (chloroform ($CHCl_3$) and / or glutaraldehyde ($C_5H_8O_2$)). The experiments were simulated in a planar photocatalytic reactor. The results showed that the removal efficiency of VOCs can be reduced at high flow rates, however a competitive adsorption phenomenon between H_2O (high humidity value) and pollutants to the active photocatalytic sites have a negative influence on the oxidation of VOCs. The high removal efficiency is obtained for 3OF/3UV-led at 2.5 cm of distance between each photocatalyst. However, this configuration had the highest number of active sites and more emitted photons. By considering the effect of relative humidity and the mass transfer step, we were able to use the bimolecular L-H kinetic (Langmuir-Hinshelwood) approach and to determine the flow independent constants L-H (k and K). Moreover, the optimal value of the relative humidity can be determined by deriving the equation model. This study demonstrated that the optical fiber immobilized TiO_2 presents good stability during its recyclability and usability. With this result,

the application of this type of photocatalyst is widened, and we expect it to be very useful in several fields.

The use of this technology for the treatment of indoor air, not only in hospitals but also in various other sectors, is expected to be deepened in the near future. In addition, with the aim of using optical fibers in the degradation of different types of air pollutants, we intend to conduct an in-depth study on the inactivation of microorganisms present in air.

References:

[1] World Health Organization (WHO). Air Quality Guidelines for Europe; World Health Organization: Geneva, Switzerland, (2000).

[2] Council of Europe Council, Directive 1999/13/EC on the limitation of emissions of volatile organic compounds due to use of organic solvents in certain activities and installations, Official Journal of the European Union, (1999), L85, 1.

[3] H. Mallawaarachchi, L. DE Silva. Green framework to improve indoor air quality in buildings: reducing the impact of sick building syndrome on office workers in Sri Lanka: a literature review. (2012).

[4] A. A. Assadi, Abdelkrim Bouzaza, Dominique Wolbert, Comparative study between laboratory and large pilot scales for VOC's removal from gas streams in continuous flow surface discharge plasma, Chemical Engineering Research and Design, 106 (2016) 308-314

[5] R. Li, Y. Huang, D. Zhu, W. Ho, J. Cao, S. Lee,. Improved Oxygen Activation over a Carbon/Co3O4 Nanocomposite for Efficient Catalytic Oxidation of Formaldehyde at Room Temperature. Environmental Science & Technology, 55 (2021), pp. 4054-4063.

[6] Y. Huang, P. Wang, Z. Wang, Y. Rao, J. J. Cao, S. Pu, W. Ho, S. C. Lee, Protonated g-C3N4/Ti3+ self-doped TiO2 nanocomposite films: Room-temperature preparation,

hydrophilicity, and application for photocatalytic NOx removal. Applied Catalysis B: Environmental, 240 (2019), pp. 122-131.

[7] P. Zhang, Y. Rao, Y. Huang, M. Chen, T. Huang, W. Ho, S. Lee, J. Zhong, J. Cao, Transformation of amorphous Bi2O3 to crystal Bi2O2CO3 on Bi nanospheres surface for photocatalytic NOx oxidation: Intensified hot-electron transfer and reactive oxygen species generation. Chemical Engineering Journal, 420 (2021), pp. 129814.

[8] P. A. Bourgeois, E. Puzenat, L. Peruchon, F. Simonet, D. Chevalier, E. Deflin, C. Brochier, C. Guillard. Characterization of a new photocatalytic textile for formaldehyde removal from indoor air. App. Catal. B: Environ., 128 (2012), pp. 171-178.

[9] M. Abidi, A. A. Assadi, B. Bouzaza, A. Hajjaji, B. Bessais, S. Rtimi. Photocatalytic indoor/outdoor air treatment and bacterial inactivation on CuxO/TiO_2 prepared by HiPIMS on polyester cloth under low intensity visible light. App. Catal. B: Environ., 259 (2019), pp. 118074.

[10] R. Katal, S. Masudy-Panah, M. Tanhaei, M. H. D. Farahani, H. Jiangyong, A review on the synthesis of the various types of anatase TiO2 facets and their applications for photocatalysis. Chemical Engineering Journal, 384 (2020) 123384.

[11] T. Zadi, A. A. Assadi, N. Nasrallah, R. Bouallouche, P. N. Tri, A. Bouzaza, M. Azizi, R. Maachi, D. Wolbert, Treatment of hospital indoor air by a hybrid system of combined plasma with photocatalysis: Case of trichloromethane. *Chem. Eng. J.*, *349* (2018), pp. 276-286.

[12] J. Zhao, X. Yang. Photocatalytic oxidation for indoor air purification: a literature review. Build. Environ. 38 (2003), pp. 645-654.

[13] N. J. Peill, M. R. Hoffmann. Development and optimization of a TiO_2-coated fiber-optic cable reactor: photocatalytic degradation of 4-chlorophenol. Environ. Sci. technol., 29 (1995), pp. 2974-2981.

[14] A. A. Azzaz, A. A. Assadi, S. Jellali, A. Bouzaza, D. Wolbert, S. Rtimi, L. Bousselmi, Discoloration of simulated textile effluent in continuous photoreactor using immobilized titanium dioxide: effect of zinc and sodium chloride. Journal of Photochemistry and Photobiology A: Chemistry, 358 (2018), pp. 111-120.

[15] R. E. Marinangeli, D. F. Ollis. Photo-assisted heterogeneous catalysis with optical fibers II. Nonisothermal single fiber and fiber bundle. AIChE J., 26 (1980), pp. 1000-1008.

[16] S. O. Gurbatov, S. A. Kulinich, A. A. Kuchmizhak, Au Nanoparticle-Decorated TiO2 Nanospheres Produced by Laser Reshaping in Water. In *Solid State Phenomena.* Trans Tech Publications Ltd 312 (2020), pp. 113-120.

[17] M. Abidi, A. Hajjaji, A. Bouzaza, K. Trablesi, H. Makhlouf, S. Rtimi, A. A. Assadi, B. Bessais. Simultaneous removal of bacteria and volatile organic compounds on Cu_2O-NPs decorated TiO_2 nanotubes: Competition effect and kinetic studies. J. Photochem. Photobiol A, 400 (2020), pp. 112722.

[18] N. L. Reddy, M. V. Shankar, S. C. Sharma, G. Nagaraju. One-pot synthesis of Cu–TiO_2/CuO nanocomposite: Application to photocatalysis for enhanced H2 production, dye degradation & detoxification of Cr (VI). Internat. J. Hydrog. Energ, 45 (2020), pp.7813-7828.

[19] H. O. N. Tugaoen, S. Garcia-Segura, K. Hristovski, P. Westerhoff. Compact light-emitting diode optical fiber immobilized TiO_2 reactor for photocatalytic water treatment. Sci. Tot. Environ., 613 (2018), pp. 1331-1338.

[20] P. WesterhoffP. Alvarez, Q. Li, J. Gardea-Torresdey, J. Zimmerman. Overcoming implementation barriers for nanotechnology in drinking water treatment. Environ. Sci., 3 (2016), pp. 1241-1253.

[21] R. E. Marinangeli, D. F. Ollis. Photoassisted heterogeneous catalysis with optical fibers: I. Isolated single fiber. AIChE Journal, 23 (1997), pp. 415-426.

[22] K. Hofstadler, R. Bauer, S. Novalic, G. Heisler. New reactor design for photocatalytic wastewater treatment with TiO_2 immobilized on fused-silica glass fibers: photomineralization of 4-chlorophenol. Environ. Sci. technol., 28 (1994), pp. 670-674.

[23] W. ChoiJ. Y. Ko, H. Park, J. S. Chung. Investigation on TiO_2-coated optical fibers for gas-phase photocatalytic oxidation of acetone. App. Catal. B,, 31 (2011), pp. 209-220.

[24] H. Joo, H. Jeong, M. Jeon, I. Moon. The use of plastic optical fibers in photocatalysis of trichloroethylene. Sol. Energy. Mat. Sol. Cell., 79 (2003), pp. 93-101.

[25] A. Danion, J. Disdier, C. Guillard, F. Abdelmalek, N. Jaffrezic-Renault. Characterization and study of a single-TiO_2-coated optical fiber reactor. App. Catal. B, 52 (2004), pp. 213-223.

[26] C. Indermühle, E. Puzenat, F. Simonet, L. Peruchon, C. Brochier, C. Guillard, C. Modelling of UV optical ageing of optical fibre fabric coated with TiO_2. App. Catal. B, 182 (2016), pp. 229-235.

[27] A. Endruweit, A. D. Alobaidani, D. Furniss, A. B. Seddon, T. Benson, M. S. Johnson, A. C. Long. Spectroscopic experiments regarding the efficiency of side emission optical fibres in the UV-A and visible blue spectrum. Opt. Las. Eng., 46 (2008), pp. 97-105.

[28] W. Abou Saoud, A. Kane, P. Le Cann, , A. Gérard, , L. Lamaa, , L. Peruchon, , A. A. Assadi, Innovative photocatalytic reactor for the degradation of VOCs and microorganism under simulated indoor air conditions: Cu-Ag/TiO_2-based optical fibers at a pilot scale. Chemical Engineering Journal, 411 (2021), p. 128622.

[29] A. Almansba, A. Kane, , N. Nasrallah, , R. Maachi, , L. Lamaa, , L. Peruchon, , A. A. Assadi, Innovative photocatalytic luminous textiles optimized towards water treatment: Performance evaluation of photoreactors. *Chemical Engineering Journal*, *416* (2021), pp. 129195.

[30] C. Brochier, D. Malhomme, E. Deflin-Brevet « Nappe textile présentant des propriétés dépolluantes par photocatalyse» -no. de délivrance FR2910341, 2008-06-27 (A1) et FR2910341, 2009-02-06 (B1), 2007.

[31] T. Zadi, M. Azizi, N. Nasrallah, A. Bouzaza, R. Maachi, D. Wolbert, S. Rtimi, A. A. Assadi, Indoor air treatment of refrigerated food chambers with synergetic association between cold plasma and photocatalysis: Process performance and photocatalytic poisoning. Chem. Eng. J., 382 (2020), pp. 122951.

[32] W. Abou Saoud, A. A. Assadi, M. Guiza, A. Bouzaza, W. Aboussaoud, A. Ouederni, I. Soutrel, D. Wolbert S.Rtimi. Study of synergetic effect, catalytic poisoning and regeneration using dielectric barrier discharge and photocatalysis in a continuous reactor: Abatement of pollutants in air mixture system. App. Catal. B, 213 (2017), pp. 53-61.

[33] W. Abou Saoud, A. A. Assadi, M. Guiza, A. Bouzaza, W. Aboussaoud, I. Soutrel, A. Ouederni, D. Wolbert, S. Rtimi. Abatement of ammonia and butyraldehyde under non-thermal plasma and photocatalysis: Oxidation processes for the removal of mixture pollutants at pilot scale. Chem. Eng. J., 344 (2018), pp. 165-172.

[34] A.A. Assadi, J. Palau, A. Bouzaza, D. Wolbert Modeling of a continuous photocatalytic reactor for isovaleraldehyde oxidation: effect of different operating parameters and chemical degradation pathway Chem. Eng. Res. Des., 91 (2013), pp. 1307-1316.

[35] S.B. Kim, S.C. Hong Kinetic study for photocatalytic degradation of volatile organic compounds in air using thin film of a TiO_2 photocatalyst Appl. Catal. B, 35 (2002), pp. 305-315

[36] J. Palau, A.A. Assadi, J.M. Penya-roja, A. Bouzaza, D. Wolbert, V. Martínez-Soria. Isovaleraldehyde degradation using UV photocatalytic and dielectric barrier discharge

reactors, and their combinations J. Photochem. Photobiol. A: Chem., 299 (2015), pp. 110-117.

[37] A. A. Assadi, A. Bouzaza, M. Lemasle, D. Wolbert. Removal of trimethylamine and isovaleric acid from gas streams in a continuous flow surface discharge plasma reactor. Chem. Eng. Res. Des., 93 (2015), pp. 640-651.

[38] F. Thevenet, O. Guaitella, E. Puzenat, C. Guillard, A. Rousseau Influence of water vapour on plasma/photocatalytic oxidation efficiency of acetylene Appl. Catal. B: Environ., 84 (2008), pp. 813-820

[39] A.M. Vandenbroucke, R. Morent, N. De Geyter, Ch. Leys Non-thermal plasmas for non-catalytic and catalytic VOC abatement J. Hazard. Mater. 195 (2011), 30-54.

[40] A.A. Assadi, A. Bouzaza, D. Wolbert Study of synergetic effect by surface discharge plasma/TiO_2 combination for indoor air treatment: sequential and continuous configurations at pilot scale J. Photochem. Photobiol. A, 310 (2015), pp. 148-154.

[41] A.A. Assadi, A. Bouzaza, M. Lemasle, D. Wolbert, Acceleration of trimethylamine removal process under synergistic effect of photocatalytic oxidation and surface discharge plasma reactor. The Canadian Journal of Chemical Engineering 93 (2015), pp.1239-124.

[42] A.A. Assadi, A. Bouzaza, S. Merabet, D. Wolbert, Modeling and simulation of VOCs removal by non-thermal plasma discharge with photocatalysis in a continuous reactor: Synergetic effect and mass transfer. Chemical Engineering Journal 258 (2014), pp.119-127.

[43] G. Zhang, Y. Liu, Z. Hashisho, Z. Sun, S. Zheng, L. Zhong. Adsorption and photocatalytic degradation performances of TiO_2/diatomite composite for volatile organic compounds: Effects of key parameters. App. Surf. Sci., (2020) p. 146633.

[44] E.J. Park, H.O. Seo, Y.D. Kim Influence of humidity on the removal of volatile organic compounds using solid surfaces. Catal. Today, 295 (2017), pp. 3-13.

[45] A. Haghighat mamaghani, F. Haghighat, C. S. Lee. Performance of various commercial TiO_2 in photocatalytic degradation of a mixture of indoor air pollutants: Effect of photocatalyst and operating parameters. Sci. Technol. Built Environ., 25 (2019), pp. 600-614.

[46] T.N. Obee, R.T. Brown, TiO_2 photocatalysis for indoor air applications: effects of humidity and trace contaminant levels on the oxidation rates of formaldehyde, toluene, and1 3-butadiene. Environ. Science and Technol., 29 (1995), pp .1223-1231

[47] A. A. Assadi, A. Bouzaza, I. Soutrel, P. Petit, K. Medimagh, D. Wolbert, A study of pollution removal in exhaust gases from animal quartering centers by combining photocatalysis with surface discharge plasma: From pilot to industrial scale, Chemical Engineering and Processing: Process Intensification, 111 (2017) 1-6

[48] M. S. Li, S. C. Wu, Y. H. Peng, Y. H. Shih, Adsorption of volatile organic vapors by activated carbon derived from rice husk under various humidity conditions and its statistical evaluation by linear solvation energy relationships. Separat. Purif. Technol., 170 (2016) pp. 102-108.

[49] O. Debono, V. Hequet, L. Le Coq, N. Locoge, F. Thevenet. VOC ternary mixture effect on ppb level photocatalytic oxidation: Removal kinetic, reaction intermediates and mineralization. App. Catal. B: Environ., 218 (2017), pp. 359-369.

[50] J. Chen, G. Li, Z. He, T. An. Adsorption and degradation of model volatile organic compounds by a combined titania–montmorillonite–silica photocatalyst. J. Hazard. Mat., 190 (2011), 416-423.

[51] A. H. Mamaghani, F. Haghighat, C. S. Lee. Photocatalytic degradation of VOCs on various commercial titanium dioxides: Impact of operating parameters on removal efficiency and by-products generation. Build. Environ., 138 (2018), pp. 275-282.

[52] P. Kalliokoski, P. Luscuere, A. Streinfel, Indoor air quality in hospitals and other health care facilities. ISIAQ task force reports. ISIAQ, (2003).

[53] L. Zhang, W.A. Anderson, S. Sawell, C. Moralejo, Mechanistic analysis on the influence of humidity on photocatalytic decomposition of gas-phase chlorobenzene. Chemos., 68 (2007), pp. 546-553.

[54] W. Abou Saoud, A.A. Assadi, M. Guiza, S. Loganathan, A. Bouzaza, W. Aboussaoud, A. Ouederni, S. Rtimi, D. Wolbert, Synergism between non-thermal plasma and photocatalysis: implications in the post discharge of ozone at a pilot scale in a catalytic fixed-bed reactor, Appl. Catal. B 241 (2019), pp. 227–235.

[55] A. Queffeulou, L. Geron, E. Schaer Prediction of photocatalytic air purifier apparatus performances with a CFD approach using experimentally determined kinetic parameters Chem. Eng. Sci., 65 (2010), pp. 5067-5074.

[56] A. A. Assadi, S. Loganathan, P. N. Tri, S. Gharib-Abou Ghaida, A. Bouzaza, A. N. Tuan, D. Wolbert. Pilot scale degradation of mono and multi volatile organic compounds by surface discharge plasma/TiO_2 reactor: Investigation of competition and synergism. Journal of hazardous materials, 357 (2018), pp. 305-313.

[57] M. Singh, I. Salvadó-Estivill, G. Li Puma Radiation field optimization in photocatalytic monolith reactors for air treatment AIChE J., 53 (2007), pp. 678-686.

[58] Q. Geng, Q. Guo, X. Yue Adsorption photocatalytic degradation kinetics of gaseous cyclohexane in an annular fluidized bed photocatalytic reactor. Indust. Eng Chem. Res., 49 (2010), pp. 4644-4465.

[59] Assadi, A. A., Bouzaza, A., Wolbert, D. (2012). Photocatalytic oxidation of trimethylamine and isovaleraldehyde in an annular reactor: influence of the mass transfer and the relative humidity. J. Photochem. Photobiol. A: Chem., 236 (2012), pp. 61-69.

[60] G. Costa, A.A. Assadi, S. Gharib-Abou Ghaida, A. Bouzaza, D. Wolbert, Study of butyraldehyde degradation and by-products formation by using a surface plasma discharge in pilot scale: Process modeling and simulation of relative humidity effect. Chemical Engineering Journal 307 (2017), pp. 785-792

[61] D. Chen, F. Li, A.K. Ray Effect of mass transfer and catalyst layer thickness on photocatalytic reaction. AIChE J., 46 (2000), pp. 1034-1045

[62] R. Yang, Y. Zhang, Q. Xu, J. Mo A mass transfer based method for measuring the reaction coefficients of a photocatalyst Atmos. Environ., 41 (2007), pp. 1221-1229.

[63] Y. Luo, D.F. Ollis Heterogeneous photocatalytic oxidation of trichloroethylene and toluene mixtures in air: kinetic promotion and inhibition time-dependent catalyst activity. J. Catal., 163 (1996), pp. 1-11.

[64] L. Khezami, P. Nguyen-Tri, W. Abdou Saoud, A. Bouzaza, A.El Jery, D. D. Nguyen, V. K. Gupta, A. A. Assadi,Recent progress in air treatment with combined photocatalytic/plasma processes: A review, Journal of Environmental Management, 299 (2021), pp.113588

[65] E. Shashi Menon, in Transmission Pipeline Calculations and Simulations Manual, Gulf Professional Publishing (2014).

[66] R.H. Perry, D. Green, J.O. Maloney Perry's Chemical Engineers's Handbook (7th ed.), Mc Graw-Hill Book Company, New-York (1997).

[67] J. Shang, W. Li, Y. Zhu Structure and photocatalytic characteristics of TiO_2 film photocatalyst coated on stainless steel webnet. J. Molecul. Catal. A: Chem., 202 (2003), pp. 187-195.

[68] F. Petronella, S. Rtimi, R. Comparelli, R. Sanjines, C. Pulgarin, M. L. Curri, J. Kiwi, Uniform TiO2/In2O3 surface films effective in bacterial inactivation under visible light, J. Photochem. Photobiol. A: Chem. 279 (2014) 1-7.

[69] I. Milosevic, A. Jayaprakash, B. Greenwood, B. van Driel, S. Rtimi, P. Bowen, Synergistic effect of Fluorinated and N doped TiO2 nanoparticles leading to different microstructure and enhanced photocatalytic bacterial inactivation, Nanomaterials 7 (2017) 391.

[70] I. Milošević, A. Jayaprakash, B. van Driel, B. Greenwood, A. Aimable, M. Senna and P. Bowen, Synthesis and characterization of fluorinated anatase nanoparticles and subsequent N-doping for efficient visible light activated photocatalysis, Colloids and Surfaces B: Biointerfaces 171 (2018) 445-450.

Graphical abstract

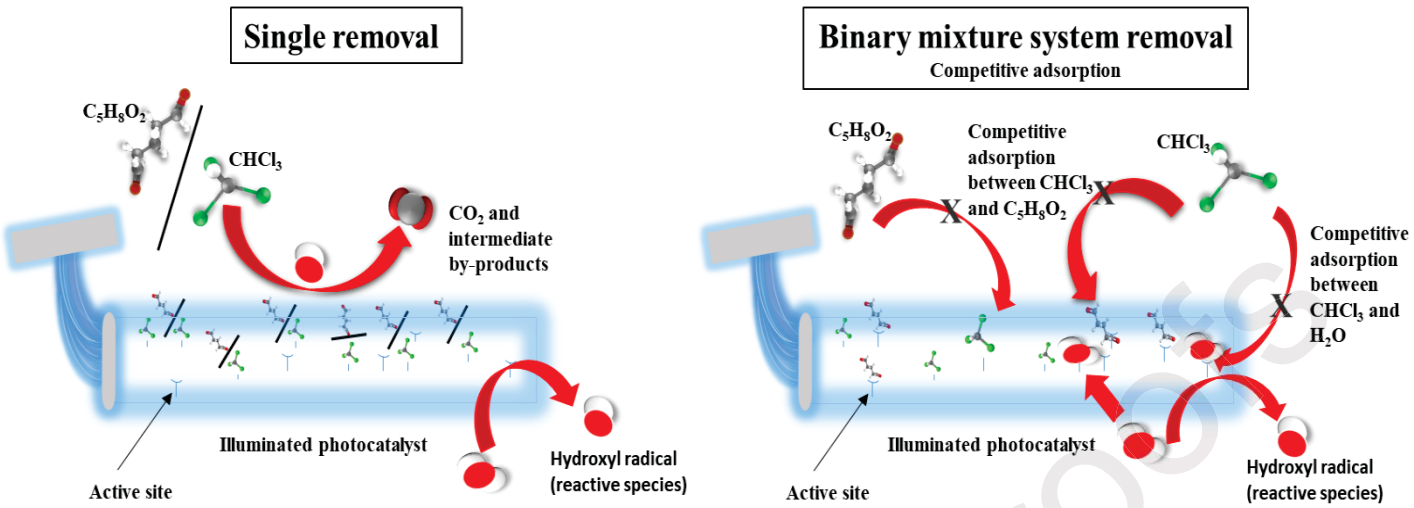

Highlights

- Proposal of a potential method of treating indoor air in hospitals
- Degradation of VOCs in a binary mixture system by TiO2 on Luminous textile.
- Testing the impacts of key parameters on the photocatalytic performance.
- Kinetic modelling and mass transfer limitation were investigated.